HHS Public Access

Author manuscript

Mol Cancer Ther. Author manuscript; available in PMC 2020 August 01.

Published in final edited form as:

Mol Cancer Ther. 2020 February ; 19(2): 602–613. doi:10.1158/1535-7163.MCT-17-0256.

Amplification of the mutation-carrying BRCA2 allele promotes RAD51 loading and PARP inhibitor resistance in the absence of reversion mutations.

Pyoung Hwa Park[1,#], **Tomomi M. Yamamoto**[2,#], **Hua Li**[1], **Allen L. Alcivar**[3], **Bing Xia**[3], **Yifan Wang**[4], **Andrea J. Bernhardy**[4], **Kristen M. Turner**[5], **Andrew V. Kossenkov**[1], **Zachary L. Watson**[2], **Kian Behbakht**[6], **Silvia Casadei**[7], **Elizabeth M. Swisher**[7], **Paul S. Mischel**[5], **Neil Johnson**[4], **Benjamin G. Bitler**[2,*]

[1]Gene Expression and Regulation Program, The Wistar Institute, Philadelphia, PA 19104, USA

[2]Division of Reproductive Sciences, The University of Colorado, Aurora, CO 80045, USA

[3]Department of Radiation Oncology, The Cancer Institute of New Jersey, Rutgers University, New Brunswick, NJ 08901, USA

[4]Molecular Therapeutics Program, Fox Chase Cancer Center, PA 19111, USA

[5]Moores Cancer Center, University of California at San Diego, La Jolla, California 92093,USA

[6]Division of Gynecologic Oncology, The University of Colorado, Aurora, CO 80045, USA

[7]Department of Ob/Gyn, University of Washington, Seattle, WA 98195, USA

Abstract

Patients harboring germline Breast Cancer susceptibility genes 1 and 2 (BRCA1/2) mutations are predisposed to developing breast, pancreatic, and ovarian cancers. BRCA2 plays a critical role in homologous recombination DNA repair and deleterious mutations in *BRCA2* confer sensitivity to poly(ADP-ribose) polymerase (PARP) inhibition. Recently, the PARP inhibitors olaparib and rucaparib were FDA approved for the treatment of metastatic breast cancer and recurrent ovarian cancer patients with mutations in BRCA1/2. Despite their initial anti-tumor activity, the development of resistance limits the clinical utility of PARP inhibitor therapy. Multiple resistance mechanisms have been described, including reversion mutations that restore the reading frame of the *BRCA2* gene. In this study, we generated olaparib and rucaparib resistant *BRCA2* mutant Capan1 cell lines. We did not detect secondary reversion mutations in the olaparib or rucaparib resistant clones. Several of the resistant clones had gene duplication and amplification of the mutant *BRCA2* allele, with a corresponding increase in expression of a truncated BRCA2 protein. In addition, homologous recombination (HR)-mediated DNA repair was rescued, as evidenced by the restoration of RAD51 foci formation. Using mass spectrometry, we identified Disruptor Of Telomeric silencing 1-Like (DOT1L), as an interacting partner of truncated BRCA2. RNA-

[*]Corresponding author: Benjamin G. Bitler, Ph.D., 12700 East 19th Avenue, MS 8613, Aurora, CO 80045, USA, Benjamin.bitler@cuanschutz.edu, Phone: (303) 724-0574.
[#]Authors contributed equally to this work

The authors declare no potential conflicts of interest.

interference-mediated knockdown of *BRCA2* or *DOT1L* was sufficient to re-sensitize cells to olaparib. The results demonstrate that independent of a *BRCA2* reversion mutation amplification of a mutant-carrying *BRCA2* contributes to PARP inhibitor resistance.

INTRODUCTION

Germline mutations in the *BRCA1* or *BRCA2* genes significantly increase an individual's life-time risk of developing breast, prostate, and ovarian cancer [Reviewed in (1)]. The BRCA1 and BRCA2 proteins play essential roles in homologous recombination (HR)-mediated repair of DNA double-strand breaks. BRCA1 has been implicated in DNA end resection as well as RAD51 loading, whereas BRCA2 is considered essential for RAD51 loading onto resected single stranded DNA [reviewed in (2)]. Additionally, both proteins prevent excessive MRE11-mediated degradation of DNA replication forks (3). Thus, BRCA1/2 play critical roles in maintaining genome stability.

Cancers with mutations that disrupt BRCA1/2 protein activity are highly sensitive to treatment with inhibitors of poly(ADP)-ribose polymerase (PARP). The PARP inhibitors (PARPi) olaparib and rucaparib are now approved for the treatment of BRCA1/2 wildtype and mutated ovarian cancers and BRCA1/2-mutated breast cancers [reviewed in (4)] (5). While not yet approved for pancreatic cancer, a clinical trial reported that olaparib maintenance significantly extended progression free survival (6). However, PARPi resistance poses a significant clinical challenge and is understudied in the context of pancreatic cancer (7). Previously described mechanisms of PARPi resistance include: secondary mutations in the *BRCA2* gene that restore the open-reading frame, increased p-glycoprotein expression, elevated expression of mutated BRCA1 proteins, stabilization of the replication fork, and loss of DNA end resection inhibitory proteins such as 53BP1 (8–12). Notably, most of these mechanisms have only been demonstrated *in vitro*. Notwithstanding these observations, there are other routes to PARPi resistance.

The Capan1 cell line was derived from a pancreatic adenocarcinoma and harbors a single-base pair deletion in exon 11 (r.6174del) of the *BRCA2* gene, which is found at an elevated frequency in the Ashkenazi Jewish population and is associated with an increased risk of breast, ovarian, and pancreatic cancers (13–15). Mutations within the region of exon 11 of the *BRCA2* gene result in a premature stop codon. If mRNA is successfully translated, the BRCA2 protein generated would be predicted to lack the C-terminal DNA binding domain, but retain 7 of the 8 BRC motifs that are needed for RAD51 loading onto DNA (16). Capan1 cells have been characterized as being HR-deficient with low basal levels of RAD51 foci (17). Previous studies have generated cisplatin- and olaparib-resistant Capan1 derivatives and showed that cells acquire secondary reversion mutations that restored the *BRCA2* reading frame and were responsible for generating a functional BRCA2 protein, capable of promoting HR and therapy resistance (18,19).

In this report, we utilized two independent PARPi to generate multiple Capan1 resistant derivatives. Secondary mutations were not detected in the *BRCA2* gene. Rather, there was a gain in gene copy number of the mutation-carrying *BRCA2* allele that correlated with an increase of a truncated BRCA2 protein. Knockdown of *BRCA2* resensitized resistant

Capan1 cells to PARPi. Resistant cells with BRCA2 amplification had an increase in histone H3 lysine 79 methylation (H3K79Me) and subsequent *BRCA2* knockdown reduced Disruptor of Telomeric silencing 1-like (DOT1L). The findings of this report offer a novel mechanism of PARPi resistance that is mediated through the amplification mutated *BRCA2*.

MATERIALS AND METHODS

Cell culture, and PARP inhibitor resistance establishment

Capan-1 and MDA-MD-231 (positive control for wildtype BRCA2) were purchased from the American Type Culture Collection. TOV-21G (positive control for wildtype BRCA2) from Japanese Cancer Research Resources Bank, and DLD-1 from Horizon (#HD 105-007). Cells were cultured in RPMI1640 with 10% fetal bovine serum and 1% penicillin/ streptomycin. Capan-1 olaparib and rucaparib resistant cell line was established by a stepwise exposure to increasing concentrations of olaparib from 15 nM to 128 μM. The established resistant cells were maintained in 2 μM olaparib. Cells lines were cultured for a maximum of 8 weeks and monthly tested for mycoplasma using LookOut Mycoplasma PCR based kit (Sigma, cat. # MP0035). Capan-1 and DLD-1 cells were most recently tested on July 2nd 2019 and July 22nd 2019, respectively. Cell lines were authenticated at University of Arizona Genetics Core via small tandem repeat.

Reagents and Antibodies

Olaparib (AZD2281), rucaparib, and pinometostat (EPZ5676) were obtained from Selleckchem. The following antibodies and reagents were obtained from the indicated suppliers: anti-BRCA2 (Bethyl Laboratories, cat. No. A311-267A, 1:5000), anti-BRCA2 ab-1 (Millipore, cat. No. OP95, 1:1000), anti-BRCA2 ab-2 (Millipore, cat. No. CA1033), anti-β-actin (Sigma, cat. No. A1978), anti-GAPDH (Millipore, cat. No. MAB374, 1:20000), anti-DOT1L (Cell Signaling, cat. No.77087), anti-RAD51 (Millipore, cat. No. ABE257 1:500), and anti-BRCA1 (Calbiochem, cat. No. OP92, 1:500), anti-phospho-γH2AX (Ser139) (Millipore, cat. No. 05-636, 1:400), anti-Vinculin (Cell signaling, cat. No. 13901, 1:1000), anti-H3K79Me (Abcam, cat. No. Ab177185 1:1000) and anti-BrdU (BD Biosciences, cat. No. 347583).

Lentivirus

Lentiviral constructs were packaged using the Virapower Kit and as described previously (20,21). pLKO.1, pLKO.1-shBRCA2 #1 (TRCN0000040194) and pLKO.1-shBRCA2 #2 (TRCN0000040197) were obtained from at the Wistar Institute. shDOT1L #1 (TRCN0000236343) and shDOT1L #2 (TRCN0000236345) were obtained from Functional Genomics Facility at the University of Colorado Denver. Dr. Neil Johnson's laboratory developed pLenti-IRES-GFP-mCherry, pLenti-IRES-GFP-Full Length BRCA2, and pLenti-IRES-GFP-Truncated BRCA2 plasmids. Following pLenti-IRES-GFP transduction GFP positive cells were sorted twice to establish stable cell lines.

Reverse-transcriptase quantitative PCR and RNA Sequencing

RNA was isolated from cells with RNeasy Mini Kit (Qiagen) followed by on-column RNase-free DNase I treatment (Qiagen). *BRCA2* expression (FWD, 5'-

GGGAAGCTTCATAAGTCAGTC-3', and REV, 5'-TTTGTAATGAAGCATCTGATACC-3') was determined using SYBR green 1-step iScript kit (Bio-Rad) on a Bio-Rad Chromo4 machine. β-2-microglobulin (*B2M*) was used as an internal control (FWD, 5'-GGCATTCCTGAAGCTGACA-3', and REV, 5'-CTTCAATGTCGGATGGATGAAAC-3'). *DOT1L* expression (FWD, 5'-CACCAGACTGACCAACTCGC -3' and REV, 5'-TCCTAGTTACCTCCAACTGTGC-3') was determined using Luna universal One-Step RT-qPCR kit (New England Biolabs). Isolated RNA was utilized for global next-generation sequencing (RNA-seq) at The Wistar Genomics Facility. RNA-seq data (GSE86394) was aligned with bowtie2 (22) algorithm and RSEM v1.2.12 software (23) was used to estimate read counts and FPKM values on transcript level using Ensemble transcript information. DESeq algorithm (24) was used to compare two conditions and differences of at least 2 fold that passed False Discovery Rate (FDR)<15% threshold were considered significant. Single nucleotide polymorphisms (SNP) were called using VarScan2 software and annotated using SnpEff tool (25,26). Results that had $p<0.001$ by Fisher Exact Test differences and FDR<15% between resistant and parental cells were considered significant.

DNA sequencing

Genomic DNA from cell line rucaparib resistant subclones were sequenced with the BROCA-HRv7 targeted sequencing assay as previously described (27). BROCA-HR includes 81 DNA repair genes. The known *BRCA2* mutation site was sequenced with Sanger sequencing.

Colony formation assay

Cell lines were transduced with pLKO.1-shBRCA2 (#1 or #2), pLKO.1-shDOT1L (#1 or #2) or pLKO.1-control followed by puromycin selection (1 μg/mL). Cells were seeded in 24-well plates. Indicated doses of compounds were added and cell medium with compounds was refreshed every three days. Cells were cultured for 12 days. Colonies were fixed with 10% methanol/10% acetic acid. Colonies were stained with 0.5% crystal violet. Colonies were counted using ImageJ Software or dissolved into fixation buffer (10% methanol, 10% acetic acid, PBS) and optical density (570 nm) measured.

Copy number variation assay

Total genomic DNA was isolated from cells with Quick-gDNA Universal Kit (Zymo Research). Copy number variation was determined using pre-designed BRCA2 primers (Life Technologies, cat. No. 440291) and TaqMan Genotyping Mastermix (Life Technologies). TaqMan Copy Number Reference Assay, Human RNase P (Life Technologies, cat. No. 4403326) was used as an internal control.

Immunoblotting

Cells were collected with sample buffer (2% SDS, 10% glycerol, 62.5mM Tris, pH 8.0, 0.25% Bromophenol Blue, and 100 mM DTT) or RIPA buffer (150 mM NaCl, 1% NP-40, 0.5% sodium deoxycholate, 0.1% SDS, and 50 mM Tris-HCl pH 8.0) supplemented with Complete protease inhibitor cocktail (Roche). Protein concentrations were measured via

BCA kit (Pierce, Cat#23225). Protein samples were separated on SDS-PAGE and transferred on PVDF membrane. Membranes were incubated in primary antibody, followed by either incubating with HRP linked anti-IgG antibodies and detected with chemiluminescent substrate (Thermo Fisher Scientific), or IRDye conjugated anti-IgG antibodies (Li-Cor) and detected with Odyssey digital fluorescence system (Li-Cor).

Histone Extraction

Histones were extracted from cells using the Abcam extraction kit (ab113476) per the manufacturer's protocol.

Immunoprecipitation

Cell pellets were suspended into 500 μl of Buffer A (10 mM HEPES, 1.5 mM MgCl2, 10 mM KCl, 0.5 mM DTT, 0.05% NP40, Complete protease inhibitor [Roche] and phosphatase inhibitors [10 mM NaF and 0.2 mM Na_3VO_4], pH 7.9) at 4°C. Using 1 mL syringe passed cell suspension through a 26G needle 10X. Incubate lysate at 4°C for 15 min and centrifuge at 720 x g for 5 min at 4°C. The cell pellet was suspended into 374 μl of Buffer B (5 mM HEPES, 1.5 mM MgCl2, 0.2 mM EDTA, 0.5 mM DTT, 26% glycerol (v/v), Complete protease inhibitor and phosphatase inhibitors, pH 7.9) and 26 μl of 4.6 M NaCl. The pellet was homogenized with disposable pestle and incubated at 4°C for 30 min, and centrifuged at maximum speed (13,000 x g) for 20 min at 4°C. Supernatant was collected, sonicated for 10 sec (Branson Sonifier 250, 20% Duty Cycle, 2 output control), and used for the immunoprecipitation. Protein concentration was measured using a BCA kit (Pierce, Cat#23225), and 50 μg-75 μg of protein was used for immunoprecipitation.

N-terminus targeting anti-BRCA2 (Bethyl Laboratories, cat. No. A303-434A) or rabbit IgG (Santa Cruz, cat. No. SC-2027) was added to protein samples with Dynabeads protein A (Thermo Fisher Scientific). Samples were incubated on a rotator and the beads were washed with NETN buffer (100 mM NaCl, 20 mM Tris-Cl, pH 8.0, 0.5 mM EDTA, 0.5% NP-40). Proteins were eluted with 1X sample buffer. Eluted samples were separated on SDS-PAGE and transferred on PVDF membrane. Each immunoprecipitation set of samples was incubated with isotype control (IgG), N-terminus targeting anti-BRCA2 antibody (Ab-1, Bethyl Laboratories, cat. No. A303-434A, 1:5000), C-terminus targeting anti-BRCA2 antibody (Ab-2, Bethyl Laboratories, cat. No. A303-435A, 1:5000) or anti-DOT1L antibody (Cell Signaling,1:1000).

Mass Spectrometry

Capan-1 and Capan-1-OR cells were irradiated at 5 Gy, collected 4 hrs after irradiation, and cells were lysed in ice-cold IP lysed buffer (50 mM Tris-HCl, pH 8.0, 1 mM EDTA, 0.5% TritonX-100, 150 mM NaCl, Complete protease inhibitor (Roche), 10 mM NaF, 0.2 mM Na_3VO_4). Cells were sheared using a 26G needle. Lysates were incubated on ice for 30 min and were centrifuged at 17,000 x g for 20 min at 4°C. The concentration of the supernatant was determined with a BCA protein and 3.2 mg from Capan-1 or 16 mg from Capan-1-OR cells of total protein were used for immunoprecipitation. After being pre-cleared with 75 μl of protein A beads (NEB, Cat# 91425) that had been pre-equilibrated with IP lysis buffer for 30 min at 4°C, lysates incubated with either 15 μl of 1 mg/ml anti-BRCA2 antibody (Bethyl

laboratory Inc., Cat# A303-434A) or control normal Rabbit IgG (1mg/ml, R&D, Cat# AB-105-C) overnight at 4°C. Protein A magnetic beads were added and incubated for 1 hour at 4°C. Beads were washed with IP lysis buffer 3X for 10 min each at 4°C, and proteins were eluted with 2x Laemmli sample buffer (Bio-rad) and boiled for 10 min. 3 μl of the elution were used for immunoblot. 30 μl were used for 4-20% SDS-PAGE (Bio-Rad) and stained with Imperial Protein Stain (Thermo Fisher). The stained gel was processed by the University of Colorado Biological Mass Spectrometry Core Facility.

Immunofluorescence

Cells were treated with 5 Gy irradiation and incubated for 4 hrs or 3 μM olaparib for 48 hrs prior to immunofluorescence staining. Cells were fixed in 4% paraformaldehyde and permeabilized in 0.5% NP-40. Samples were incubated with antibodies against BRCA1, phospho-γH2AX (Ser139) and RAD51 followed by secondary antibodies (Invitrogen). Slides were mounted with prolong anti-fade reagent (Invitrogen), images were captured on a Nikon Fluorescence microscope and analyzed using NIS-Elements software (Nikon).

Fluorescence in situ hybridization

Capan1 and Capan1-RR cells were arrested in metaphase by colcemid treatment (0.1 μg/ml) for 2 hrs. Cells in metaphase were subsequently collected and incubated in 0.075 M KCl for 10 min, followed by 3 washes in Carnoy's fixative (3:1 methanol: glacial acetic acid). Interphase nuclei and cells in metaphase were dropped onto humidified glass slides, aged overnight, and FISH was performed by immersing slides in ascending ethanol series (70%, 80%, and 100%) for 2 min. *BRCA2* FISH probe (Empire Genomics) was applied to slides, and the cellular DNA and FISH probes were co-denatured at 75°C for 3 min. Hybridization was then carried out overnight at 37°C, followed by washing in 0.4X saline-sodium citrate buffer (SSC) and 2X SSC / 0.1% Tween-20. SSC diluted from a 20X stock solution (3 M NaCl, 0.3 M sodium citrate, pH 7). Anti-fade mounting medium with DAPI was applied to the slide, and cells in metaphase were imaged with an Olympus BX43 fluorescent microscope equipped with a QIClick camera.

Statistical Analysis

Statistical analysis was performed using GraphPad Prism (Prism 8). Two-tailed student *t-test* or ANOVA were utilized to calculate p-value. All quantitative data are graphed as mean with standard error mean (S.E.M). A calculated p-value of less than 0.05 was considered significant.

RESULTS

Derivation of PARP inhibitor resistant cell lines.

To identify mechanisms of PARPi resistance in a pancreatic cell model, we examined Capan1 cells. Capan1 cells have a single-base pair deletion in exon 11 (r.del6174 or 6174delT) of the *BRCA2* gene, which is predicted to produce a protein containing the RAD51 binding sites (BRC-repeats) and lacking the DNA binding domain (Fig. 1A). Examination of The Cancer Genome Atlas detected 35 tumor types and 269 individual tumors with a *BRCA2* mutation beyond the BRC repeats (Table 1). Furthermore, 20 tumor

types and 11.8% of tumors with *BRCA2* mutations are predicted to results in a truncated protein lacking the DNA binding domain, which recapitulates the 6174delT mutation (Table 1). To establish resistance, Capan1 cells were incubated with increasing concentrations of either olaparib or rucaparib. Initially, we examined a heterogeneous population of olaparib resistant cells (Capan1-OR-Het). To confirm resistance, colony formation assays on Capan1 and Capan1-OR-Het cells were performed using increasing concentrations of olaparib. We observed the Capan1-OR-Het cells were an average of 743-fold ($p<0.0001$) more resistant compared to the Capan1 parental population (Fig. 1B–C). Capan1-OR-Het cells were also an average of 1000-fold resistant to rucaparib (Fig. S1A). Colony formation assays revealed changes in proliferation rates between Capan1 and Capan1-OR-Het cells, which was confirmed via cell counting and BrdU incorporation assays (Fig. S1B–D).

PARPi resistance can be associated with cross-resistance to additional DNA damaging agents, including cisplatin (18). We observed that Capan1-OR-Het cells were 110-fold ($p=0.0036$) more resistant to cisplatin compared to Capan1 (Fig. 1D–E). In contrast, we examined the response of Capan1-OR-Het cells to a microtubule stabilization agent, docetaxel, and found Capan1 and Capan1-OR-Het cells displayed similar sensitivities (Fig. 1F–G). To limit genetic heterogeneity, we established clonal populations from Capan1-OR-Het cells, referred to as Capan1-OR-1 and -2. Utilizing colony formation assays, we observed Capan1-OR-1 and 2 cells were an average of 387 and 279-fold ($p<0.0001$ and $p<0.0001$) resistant to olaparib compared to Capan1 cells (Fig. 1H). Similar results were obtained with Capan1 cells cultured in the presence of an independent PARPi, rucaparib, and seven individual resistant (Capan1-RR) sub-clones were developed. All of the subclones were observed to be highly resistant to rucaparib, olaparib, and cisplatin (Fig. S1E–G). These data demonstrate that the Capan1 rucaparib and olaparib resistant cells are cross-resistant to other PARPi and platinum-based agents.

Examination of resistant clones for BRCA2 secondary mutations.

Previous studies showed that olaparib and cisplatin resistance results from the upregulation of p-glycoprotein or secondary mutations that restore the open-reading frame (ORF) of the *BRCA2* gene (11,18,19). We examined changes in functional efflux activity in Capan1 versus resistant clones. We did not observe a significant difference between Capan1 and resistant clones for the rate of drug efflux based on doxorubicin release assays (Fig. S2A). To further investigate the mechanism of PARPi resistance, we performed next generation sequencing of total RNA (RNA-seq) isolated from parental and Capan1-OR-Het cells (GEO: GSE86394). p-glycoproteins were not differentially upregulated in the Capan1-OR-Het cells compared to the parental cells (Table S1). Examination of *BRCA2* single nucleotide polymorphisms (SNPs) allele frequencies between Capan1-OR-Het and Capan1 cells did not detect any changes suggesting there was not a reversion event (Table S2). Furthermore, Sanger sequencing of DNA from Capan1-OR-1 and -2 for BRCA2 reversion mutations did not detect reversions in the region of the 6174delT (Fig. S2B). In Capan1-RR cells, we assessed *BRCA2* mutational status by examination of genomic DNA *via* BROCA-HR testing (27). We detected the original *BRCA2* (r.del6174) mutation but no other *BRCA2* mutations. Furthermore, there were no new mutations in DNA repair genes in the resistant clones compared to parental cells including *TP53BP1, CHD4*, or other genes that might

confer resistance (Fig. S2C). The lack of *BRCA2* reversion mutations and efflux activity indicate these mechanisms are not playing a role in PARPi resistance.

Immunoprecipitation analysis of BRCA2.

To further ensure a BRCA2 reversion event had not occurred, we evaluated total BRCA2 protein levels. We immunoprecipitated (IP) BRCA2 using antibodies that recognize the epitopes before (Ab-1) and after (Ab-2) the predicted truncation (Fig. S3A). As a control for antibody specificity, we transduced Capan1-OR-2 with two short-hairpins specific for *BRCA2* (shBRCA2). In the Capan1-OR-1 IP, we did not detect full-length BRCA2, but observed an increase in a truncated form (Fig. 2A–B and S3B). In the rucaparib resistant sub-clones 8 and 13, Ab-1 was utilized for BRCA2 IP. We observed that the truncated form of BRCA2 was IPed from the two sub-clones compared to Capan1, and was only detected by Ab-1, not by Ab-2 (Fig. 2C). In addition, we detected an interaction of the truncated form of BRCA2 with two mediators of HR, PALB2 and RAD51 (Fig. 2C). These data demonstrate that *BRCA2* reversion was not observed in Capan1 PARPi resistant clones, but there was an increase in truncated BRCA2 expression, and BRCA2 interacted with HR proteins.

Amplification of mutated BRCA2.

RNA-seq analysis revealed a significant increase in the number of aligned reads to the *BRCA2* gene in the resistant cells compared to Capan1 cells (7585 vs. 1381, Fig. 3A and Table S1). mRNA overexpression was confirmed by quantitative PCR of *BRCA2* in Capan1 parental and resistant (Capan1-OR-Het, -1 and -2) populations (Fig. 3B). In both Capan1-OR and –RR cells, we observed that the clones overexpress the truncated BRCA2 protein (Fig. 3C and S3C). Not all of the Capan1-RR cells had an increase in BRCA2 expression, but clones 8 and 13 had the highest truncated BRCA2 expression. Genomic localization of differentially expressed genes showed an enrichment of upregulated genes on chromosome 13q (Fig. 3D) suggesting a chromosomal aberration. Given this observation and increase in both mRNA and protein expression, using a PCR based approach we examined changes in the *BRCA2* gene copy number. In the Capan1-OR cells, *BRCA2* gene copy number was significantly increased in Capan1-OR-1 and -2 compared to parental Capan1 cells (9.9 [$p=0.0004$] and 13.32 [$p<0.0001$]; Fig. 3E). *BRCA2* copy number gain was also confirmed in Capan1-RR-8 and RR-13 (4.21 [$p=0.0024$] and 6.05 [$p=0.0002$]; Fig. 3F). Furthermore, fluorescence in situ hybridization (FISH) on Capan1 and Capan1-RR clones (# 8 and 13) demonstrated multiple *BRCA2*-containing chromosomal rearrangements including, amplification and gene duplication (white arrows, Fig. 3G). These data indicate the truncated *BRCA2* gene is amplified and its resulting protein are overexpressed in PARPi resistant populations.

HR repair is functional in PARPi resistant cells.

PARPi resistance has been attributed to a restoration in the HR DNA repair pathway (18). We therefore evaluated the HR repair pathway response by inducing double-strand DNA breaks (DSB) through irradiating (IR; 5 Gy) Capan1 cells and Capan1-OR-1 and -2. To assess the HR repair pathway activity on a single cell level, we performed immunofluorescence analysis following IR to examine the presence of BRCA1 and RAD51

foci. We observed that IR induced a significant increase in BRCA1 foci positive cells in Capan1-OR-1, -2 clonal and heterogeneous populations compared to Capan1 cells (44.8% vs 81.5%, p=0.0317 and 44.8% vs. 79.3%, p=0.0307) (Fig. 4A–B and S4A–B). RAD51 is recruited to DSBs through BRCA2's BRC motifs to facilitate strand invasion during HR repair (28). The formation of RAD51 foci after DNA damage is an output of functional HR repair (29). IR-induced DNA damage led to a significant increase in RAD51 foci-positive cells in Capan1-OR-1, -2 clonal populations versus Capan1 cells (0% vs 22.0%, p=0.0099 and 0% vs. 23.6%, p=0.0067) (Fig. 4A–B). Similar results were observed in rucaparib resistant Capan-1 cells (Fig. S4C–D). These data suggest that the HR DNA repair pathway is functional in PARPi resistant Capan1 cells.

Modulation of truncated BRCA2.

To directly address the role truncated BRCA2 in mediating HR repair we performed loss-of and gain-of-function studies. In PARPi resistant Capan1 cells, we observed increased expression of truncated BRCA2. Therefore, we assessed the sensitivity of DNA damaging agents after knocking down truncated *BRCA2*. We transduced shControl and two independent shBRCA2 (#1 and #2) into Capan1-OR-1 and observed a varying degree of *BRCA2* knockdown (Fig. 5A–B). shControl and shBRCA2 expressing cells were utilized for colony formation assays with increasing doses of olaparib or cisplatin. We observed that knockdown of *BRCA2* in Capan1-OR-1 cells significantly restored sensitivity to olaparib by 1.7 and 20-fold (p=0.0027 and p<0.0001) (Fig. 5C). We also confirmed these findings in the Capan1-OR-Het cells (Fig. S5A–B). Next, transduction of two shBRCA2s into Capan1-RR-8 significantly restored rucaparib sensitivity by 7.5 and 44-fold (p=0.0023 and p=0.0015) (Fig. S5C). Knocking down truncated *BRCA2* significantly sensitized Capan1-OR-1 to cisplatin by 3.9 and 11.7-fold (p=0.0004 and p<0.0001) (Fig. 5D). There was a concordance of the level of *BRCA2* knockdown and degree of re-sensitization.

For the gain-of-function studies, we were unable to stably transduce full length or truncated *BRCA2* in Capan1 cells. Therefore, we stably overexpressed GFP/HA-tagged full length or truncated BRCA2 in the DLD-1 BRCA2$^{-/-}$ cell line (30). DLD-1 is a colorectal adenocarcinoma cell line that is *BRCA2* wildtype; however, cells were genetically engineered with exon 11 deleted, which results in a loss *BRCA2*$^{-/-}$ cell line (30). Following transduction into DLD-1 BRCA2$^{-/-}$ cells, we confirmed expression of both full length and truncated *BRCA2* (Fig. 5E). As expected, the DLD-1 BRCA2$^{-/-}$ expressing the full length BRCA2 lead to olaparib resistance compared to the DLD-1 BRCA2$^{-/-}$ mCherry control cells (765 nM vs. 0.462 nM, respectively) (Fig. 5F). The DLD-1 BRCA2$^{-/-}$ expressing the truncated form, however failed to promote olaparib resistance compared to the DLD-1 BRCA2$^{-/-}$ mCherry control cells (2.04nM vs. 0.462 nM, respectively) (Fig. 5F). In contrast, knockdown of truncated BRCA2 in PARPi resistant Capan1 cells led to resensitization, which suggests truncated BRCA2 in the Capan1 cells is promoting PARPi resistance through a secondary adaptation.

Truncated BRCA2 interactome.

To investigate the possibility that an additional adaptation is required to support the ability of truncated BRCA2 to promote resistance in Capan1 and Capan1-OR-2 cells, we irradiated

cells and immunoprecipitated (IP) BRCA2. Subsequently, BRCA2 interacting proteins were identified via mass spectrometry. As a loading control for the IP-mass spectrometry, non-specific tubulin and heat shock proteins were observed at similar levels between Capan1 and Capan1-OR (Table S3). Notably, BRCA2 was effectively IPed and peptide mapping of BRCA2-associated peptides failed to identify any C-terminal peptides confirming the absence of a reversion mutation (Fig. S6A). IP-mass spectrometry data was filtered based on peptide counts from the IgG non-specific pulldown and by the CRAPome prevalence (<10% of all proteomic experiments, (31)). 37 proteins differentially interact with truncated BRCA2 in Capan1-OR-2 compared to Capan1 cells (Table S3). Similar to Capan1-RR (Fig. 2C), the BRCA2 pulled down in Capan1-OR cells showed an enrichment of HR proteins, PALB2 and RAD51 (Fig. 6A). Notably, the histone methyltransferase (HMT), DOT1L, and its cofactor, MLLT10, were significantly enriched in the BRCA2 IP in Capan1-OR-2 cells compared to Capan1 cells (Fig. 6A).

DOT1L functions in a complex with its cofactor, MLLT10, and is the only enzyme known to methylate histone H3 lysine 79 (H3K79Me1/2/3) and is linked to DNA damage repair [reviewed in (32)]. In Mixed Lineage Leukemia (MLL), aberrant DOT1L and MLLT10 activity are responsible for chromosomal rearrangements (33,34). We validated the BRCA2 and DOT1L IP in Capan1-OR-Het cells (Fig. 6B). In Capan1-OR-Het cells, *DOT1L* mRNA expression was only modestly upregulated by 1.3-fold (Fig. 6C). In contrast, DOT1L protein was increased in Capan1-OR-Het cells compared to Capan1 cells, and knockdown of *BRCA2* promoted the loss of DOT1L protein (Fig. 6D). In the DLD-1 model, we evaluated DOT1L and were unable to detect protein expression in either the BRCA2-null cells or in truncated BRCA2 overexpressing cells. However, we subsequently overexpressed *DOT1L* in these cells and DOT1L protein overexpression was only observed in cells expressing truncated BRCA2 (Fig. S6B). These data provide a possible explanation as to why overexpressing truncated BRCA2 in the DLD-1 cell line failed to induce olaparib resistance.

We next wanted to assess the role of DOT1L in Capan1 PARPi resistant cells. A control and two independent shRNAs specific for *DOT1L* were transduced into Capan1-OR-Het cells. Varying levels of DOT1L knockdown were achieved (Fig. 6E) and corresponded with the loss of H3K79Me (Fig. 6F). Notably, DOT1L's enzymatic product was also decreased following *BRCA2* knockdown (Fig. 6F). In the Capan1-OR-Het cells, DOT1L #1 and #2 shRNA-mediated knockdown resensitized cells to olaparib by 2.7 and 6.1-fold, respectively (Fig. 6G). Taken together these data suggests that DOT1L and truncated BRCA2 are potentially cooperating to promote PARPi resistance.

We next determined whether the loss of DOT1L expression (shRNA) or its enzymatic activity (DOT1L inhibitor – pinometostat [EPZ5676] (35)) attenuated HR repair via RAD51 loading. *DOT1L* knockdown or inhibited cells were irradiated with 5 Gy, incubated for 4 hrs, and RAD51 foci positive cells were quantified. Similarly, *DOT1L* knockdown or inhibited cells were treated with olaparib and RAD51 foci positive cells were quantified. As previously observed in Capan1-OR cells, about 20% of cells were positive for IR-induced RAD51 foci, however in either IR or olaparib treated cells *DOT1L* knockdown significantly reduced RAD51 foci (Fig. 6H–K). Treatment with a DOT1L inhibitor reduced H3K79Me in a dose dependent fashion (Fig. S6C) and H3K79Me was significantly downregulated by 2

μM pinometostat (Fig. 6L). Doses of pinometostat used are consistent with previous literature (36–38). Treatment with 2 μM pinometostat in combination with olaparib slightly reduced olaparib's IC50 in Capan1-OR-Het cells (Fig. 6M) and attenuated RAD51 foci formation by an average of 38%, which is a lesser extent than the shRNA knockdowns, 75% reduction in RAD51 foci formation (Fig. 6N–P). These data suggests DOT1L potentially contributes to olaparib resistance by increasing DNA repair and that it could be partially through a methyltransferase independent function.

While PARPi are FDA approved for ovarian cancer they are not currently approved for BRCA-mutated pancreatic cancer. We examined DOT1L expression using the ovarian cancer TCGA data. Increased expression *DOT1L* conveyed a worse progression-free survival and was associated with resistance to the DNA damaging platinum-based chemotherapy (Fig. S6D–E). Moreover, in a previously published BRCA2-mutated PARPi resistant model of ovarian cancer (39), *DOT1L* knockdown significantly inhibited colony formation (Fig. S6F–H). These data highlight that targeting DOT1L in PARPi resistant tumors could be more broadly applicable.

DISCUSSION

PARPi (olaparib and rucaparib) have entered the clinic for the treatment of *BRCA1/2*-mutated cancers; however, the development of resistance remains a significant clinical challenge and elucidating resistance mechanisms is critical. Therefore, we established olaparib and rucaparib resistant cells in the context of a mutated form of *BRCA2*. PARPi resistant cells had an amplification of the truncated form of BRCA2, which led to an increase in mRNA and protein expression. Truncated BRCA2 was observed to interact with DNA damage repair effectors, RAD51 and DOT1L. Subsequently, knockdown of truncated *BRCA2* restored sensitivity to PARPi.

In contrast to previous reports, we did not detect *BRCA2* reversion mutations, but similarly found that HR DNA repair had been restored in resistant cells (18,19). In the original report describing olaparib-resistant Capan1 cells the authors utilized two methods for generation of resistant cells: a step-wise increase in olaparib (1 nM to 50 μM) or a constant concentration (100 nM). While reversion mutations were observed under both conditions authors noted that only with the step-wise method did they observe amplified *BRCA2* (18). Comparatively, in our study we used the step-wise method for olaparib with a higher maximum dose, suggesting that the degree of selective pressure likely mediates an alternative resistance mechanism.

In the clinical setting, several studies have detected secondary reversion mutations of *BRCA1/2*. A small study examining sixteen germline BRCA1/2 matched primary and recurrent high grade serous ovarian cancer patients detected five recurrent tumors with reversion mutations. All five patients were treated with platinum-based chemotherapy and three of the five patients had been treated with PARP inhibitors (40). The therapeutic agent (platinum-based chemotherapy or PARP inhibitors) driving the observed reversion mutations is not clear. These data suggest that although reversion mutations occur, other mechanisms are also likely playing a role in the development of systemic resistance.

In Capan1 PARPi resistant cells *BRCA2* knockdown led to olaparib and rucaparib re-sensitization. Given the significant increase in *BRCA2* copy number and significant upregulation of truncated BRCA2, we further evaluated expression of truncated BRCA2 in an independent $BRCA2^{-/-}$ cell line. Overexpression of truncated BRCA2 was not sufficient to promote resistance suggesting that in the context of amplified truncated BRCA2, Capan1 cells have potentially acquired a second adaptation to facilitate the restoration of HR repair.

We demonstrated that the HR DNA repair pathway was restored in the PARP inhibitor resistant cells measured *via* BRCA1 and RAD51 foci formation. These findings are consistent with previous reports showing the BRCA2 protein-containing BRC repeats and lacking the C-terminal domain is sufficient to interact with RAD51 (41). Through BRCA2 pull-down and mass spectrometry, we identified DOT1L as a BRCA2 associated protein. The histone methyltransferase, DOT1L, directly interacts with DNA and promotes methylation on H3K79 and is the only known methyltransferase to catalyze H3K79. DOT1L is an established mediator of cell cycle regulation and DNA double strand break repair [reviewed in (32)]. In mixed-lineage leukemia, DOT1L contributes to chromosomal rearrangements and fusions, which suggest that DOT1L could be playing an active role in the chromosomal instability in the Capan-1 PARPi resistant cells (Fig. 2H). To-date the only known “reader” of the DOT1L-dependent H3K79 methylation is the tumor suppressor p53-binding protein 1, which has established roles in dictating specific DNA repair pathways (42). The DOT1L co-factor, MLLT10, was also observed in the BRCA2 pull-down. Interestingly, knockdown of *DOT1L* promoted PARPi resensitization to a greater degree than inhibiting DOT1L methyltransferase activity. We plan to determine if DOT1L has methyltransferase independent functions that mediated PARPi resistance. In our study, we predict that truncated BRCA2 and DOT1L are interacting to increase RAD51 loading, HR-mediated DNA damage repair, and PARPi resistance. Future work will investigate the relationship between truncated BRCA2 and DOT1L interaction in DNA damage response and potentially extend our findings into BRCA-wildtype tumors.

Supplementary Material

Refer to Web version on PubMed Central for supplementary material.

ACKNOWLEDGEMENTS

We acknowledge Dr. Rugang Zhang for his invaluable support. We acknowledge Lindsay J. Wheeler and Scott H. Kaufman for their critical discussion. This work was supported by grants from the NIH/NCI to N. Johnson (R01CA214799) and B.G. Bitler (R00CA194318), and Department of Defense Awards to N. Johnson (OC140040/OC130212) and B.G. Bitler (OC170228). Research supported by a Stand Up To Cancer-Ovarian Cancer Research Fund Alliance-National Ovarian Cancer Coalition Dream Team Translational Cancer Research Grant to E.M. Swisher (SU2C-AACR-DT16-15). Stand Up To Cancer is a division of the Entertainment Industry Foundation. Research grants are administered by the American Association for Cancer Research, the Scientific Partner of SU2C. Support of Core Facilities was provided by The Wistar Institute Cancer Center Support Grant CA010815 to and the University of Colorado Cancer Center Support Grant (P30CA046934).

REFERENCES

1. Narod SA. Modifiers of risk of hereditary breast and ovarian cancer. Nat Rev Cancer 2002;2:113–23 [PubMed: 12635174]

2. Gudmundsdottir K, Ashworth A. The roles of BRCA1 and BRCA2 and associated proteins in the maintenance of genomic stability. Oncogene 2006;25:5864–74 [PubMed: 16998501]
3. Ying S, Hamdy FC, Helleday T. Mre11-dependent degradation of stalled DNA replication forks is prevented by BRCA2 and PARP1. Cancer Res 2012;72:2814–21 [PubMed: 22447567]
4. Bitler BG, Watson ZL, Wheeler LJ, Behbakht K. PARP inhibitors: Clinical utility and possibilities of overcoming resistance. Gynecol Oncol 2017;147:695–704 [PubMed: 29037806]
5. Robson M, Im SA, Senkus E, Xu B, Domchek SM, Masuda N, et al. Olaparib for Metastatic Breast Cancer in Patients with a Germline BRCA Mutation. N Engl J Med 2017;377:523–33 [PubMed: 28578601]
6. Golan T, Hammel P, Reni M, Van Cutsem E, Macarulla T, Hall MJ, et al. Maintenance Olaparib for Germline BRCA-Mutated Metastatic Pancreatic Cancer. N Engl J Med 2019;381:317–27 [PubMed: 31157963]
7. Lord CJ, Ashworth A. Mechanisms of resistance to therapies targeting BRCA-mutant cancers. Nat Med 2013;19:1381–8 [PubMed: 24202391]
8. Barber LJ, Sandhu S, Chen L, Campbell J, Kozarewa I, Fenwick K, et al. Secondary mutations in BRCA2 associated with clinical resistance to a PARP inhibitor. J Pathol 2013;229:422–9 [PubMed: 23165508]
9. Jaspers JE, Kersbergen A, Boon U, Sol W, van Deemter L, Zander SA, et al. Loss of 53BP1 causes PARP inhibitor resistance in Brca1-mutated mouse mammary tumors. Cancer Discov 2013;3:68–81 [PubMed: 23103855]
10. Ray Chaudhuri A, Callen E, Ding X, Gogola E, Duarte AA, Lee JE, et al. Replication fork stability confers chemoresistance in BRCA-deficient cells. Nature 2016;535:382–7 [PubMed: 27443740]
11. Rottenberg S, Jaspers JE, Kersbergen A, van der Burg E, Nygren AO, Zander SA, et al. High sensitivity of BRCA1-deficient mammary tumors to the PARP inhibitor AZD2281 alone and in combination with platinum drugs. Proc Natl Acad Sci U S A 2008;105:17079–84 [PubMed: 18971340]
12. Wang Y, Krais JJ, Bernhardy AJ, Nicolas E, Cai KQ, Harrell MI, et al. RING domain-deficient BRCA1 promotes PARP inhibitor and platinum resistance. J Clin Invest 2016;126:3145–57 [PubMed: 27454289]
13. Ferrone CR, Levine DA, Tang LH, Allen PJ, Jarnagin W, Brennan MF, et al. BRCA germline mutations in Jewish patients with pancreatic adenocarcinoma. J Clin Oncol 2009;27:433–8 [PubMed: 19064968]
14. Moslehi R, Chu W, Karlan B, Fishman D, Risch H, Fields A, et al. BRCA1 and BRCA2 mutation analysis of 208 Ashkenazi Jewish women with ovarian cancer. Am J Hum Genet 2000;66:1259–72 [PubMed: 10739756]
15. Struewing JP, Hartge P, Wacholder S, Baker SM, Berlin M, McAdams M, et al. The risk of cancer associated with specific mutations of BRCA1 and BRCA2 among Ashkenazi Jews. N Engl J Med 1997;336:1401–8 [PubMed: 9145676]
16. Wong AK, Pero R, Ormonde PA, Tavtigian SV, Bartel PL. RAD51 interacts with the evolutionarily conserved BRC motifs in the human breast cancer susceptibility gene brca2. J Biol Chem 1997;272:31941–4 [PubMed: 9405383]
17. Yuan SS, Lee SY, Chen G, Song M, Tomlinson GE, Lee EY. BRCA2 is required for ionizing radiation-induced assembly of Rad51 complex in vivo. Cancer Res 1999;59:3547–51 [PubMed: 10446958]
18. Edwards SL, Brough R, Lord CJ, Natrajan R, Vatcheva R, Levine DA, et al. Resistance to therapy caused by intragenic deletion in BRCA2. Nature 2008;451:1111–5 [PubMed: 18264088]
19. Sakai W, Swisher EM, Karlan BY, Agarwal MK, Higgins J, Friedman C, et al. Secondary mutations as a mechanism of cisplatin resistance in BRCA2-mutated cancers. Nature 2008;451:1116–20 [PubMed: 18264087]
20. Bitler BG, Nicodemus JP, Li H, Cai Q, Wu H, Hua X, et al. Wnt5a Suppresses Epithelial Ovarian Cancer by Promoting Cellular Senescence. Cancer Res 2011
21. Ye X, Zerlanko B, Kennedy A, Banumathy G, Zhang R, Adams PD. Downregulation of Wnt signaling is a trigger for formation of facultative heterochromatin and onset of cell senescence in primary human cells. Mol Cell 2007;27:183–96 [PubMed: 17643369]

22. Langmead B, Salzberg SL. Fast gapped-read alignment with Bowtie 2. Nat Methods 2012;9:357–9 [PubMed: 22388286]
23. Li B, Dewey CN. RSEM: accurate transcript quantification from RNA-Seq data with or without a reference genome. BMC Bioinformatics 2011;12:323 [PubMed: 21816040]
24. Anders S, Huber W. Differential expression analysis for sequence count data. Genome Biol 2010;11:R106 [PubMed: 20979621]
25. Cingolani P, Platts A, Wang le L, Coon M, Nguyen T, Wang L, et al. A program for annotating and predicting the effects of single nucleotide polymorphisms, SnpEff: SNPs in the genome of Drosophila melanogaster strain w1118; iso-2; iso-3. Fly (Austin) 2012;6:80–92 [PubMed: 22728672]
26. Koboldt DC, Zhang Q, Larson DE, Shen D, McLellan MD, Lin L, et al. VarScan 2: somatic mutation and copy number alteration discovery in cancer by exome sequencing. Genome Res 2012;22:568–76 [PubMed: 22300766]
27. Norquist BM, Brady MF, Harrell MI, Walsh T, Lee MK, Gulsuner S, et al. Mutations in Homologous Recombination Genes and Outcomes in Ovarian Carcinoma Patients in GOG 218: An NRG Oncology/Gynecologic Oncology Group Study. Clin Cancer Res 2018;24:777–83 [PubMed: 29191972]
28. Milne GT, Weaver DT. Dominant negative alleles of RAD52 reveal a DNA repair/recombination complex including Rad51 and Rad52. Genes Dev 1993;7:1755–65 [PubMed: 8370524]
29. Graeser M, McCarthy A, Lord CJ, Savage K, Hills M, Salter J, et al. A marker of homologous recombination predicts pathologic complete response to neoadjuvant chemotherapy in primary breast cancer. Clin Cancer Res 2010;16:6159–68 [PubMed: 20802015]
30. Hucl T, Rago C, Gallmeier E, Brody JR, Gorospe M, Kern SE. A syngeneic variance library for functional annotation of human variation: application to BRCA2. Cancer Res 2008;68:5023–30 [PubMed: 18593900]
31. Mellacheruvu D, Wright Z, Couzens AL, Lambert JP, St-Denis NA, Li T, et al. The CRAPome: a contaminant repository for affinity purification-mass spectrometry data. Nat Methods 2013;10:730–6 [PubMed: 23921808]
32. Wood K, Tellier M, Murphy S. DOT1L and H3K79 Methylation in Transcription and Genomic Stability. Biomolecules 2018;8
33. Bernt KM, Zhu N, Sinha AU, Vempati S, Faber J, Krivtsov AV, et al. MLL-rearranged leukemia is dependent on aberrant H3K79 methylation by DOT1L. Cancer Cell 2011;20:66–78 [PubMed: 21741597]
34. Monroe SC, Jo SY, Sanders DS, Basrur V, Elenitoba-Johnson KS, Slany RK, et al. MLL-AF9 and MLL-ENL alter the dynamic association of transcriptional regulators with genes critical for leukemia. Exp Hematol 2011;39:77–86 e1–5 [PubMed: 20854876]
35. Daigle SR, Olhava EJ, Therkelsen CA, Basavapathruni A, Jin L, Boriack-Sjodin PA, et al. Potent inhibition of DOT1L as treatment of MLL-fusion leukemia. Blood 2013;122:1017–25 [PubMed: 23801631]
36. Godfrey L, Crump NT, Thorne R, Lau IJ, Repapi E, Dimou D, et al. DOT1L inhibition reveals a distinct subset of enhancers dependent on H3K79 methylation. Nat Commun 2019;10:2803 [PubMed: 31243293]
37. Kari V, Raul SK, Henck JM, Kitz J, Kramer F, Kosinsky RL, et al. The histone methyltransferase DOT1L is required for proper DNA damage response, DNA repair, and modulates chemotherapy responsiveness. Clin Epigenetics 2019;11:4 [PubMed: 30616689]
38. Zhang W, Zhao C, Zhao J, Zhu Y, Weng X, Chen Q, et al. Inactivation of PBX3 and HOXA9 by down-regulating H3K79 methylation represses NPM1-mutated leukemic cell survival. Theranostics 2018;8:4359–71 [PubMed: 30214626]
39. Yamamoto TM, McMellen A, Watson ZL, Aguilera J, Ferguson R, Nurmemmedov E, et al. Activation of Wnt signaling promotes olaparib resistant ovarian cancer. Mol Carcinog 2019
40. Christie ELF S; Doig K; Pattnaik S; Dawson SJ; Bowtell DD Reversion of BRCA1/2 Germline Mutations Detected in Circulating Tumor DNA From Patients With High-Grade Serous Ovarian Cancer. J Clin Oncol 2017

41. Shivji MK, Davies OR, Savill JM, Bates DL, Pellegrini L, Venkitaraman AR. A region of human BRCA2 containing multiple BRC repeats promotes RAD51-mediated strand exchange. Nucleic Acids Res 2006;34:4000–11 [PubMed: 16914443]

42. Huyen Y, Zgheib O, Ditullio RA Jr., Gorgoulis VG, Zacharatos P, Petty TJ, et al. Methylated lysine 79 of histone H3 targets 53BP1 to DNA double-strand breaks. Nature 2004;432:406–11 [PubMed: 15525939]

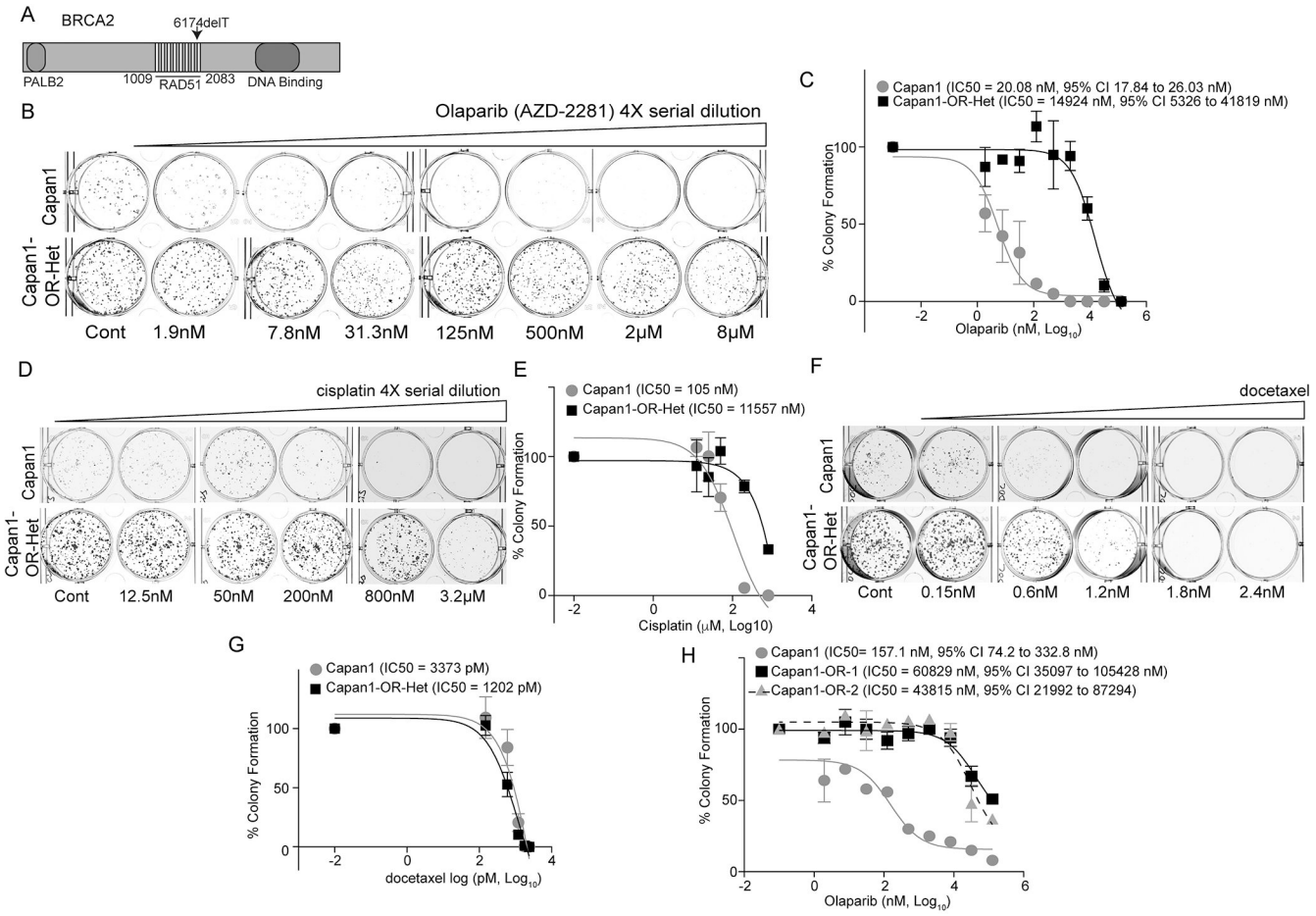

Figure 1. PARP inhibitor resistant cells are cross resistant to DNA damaging agent.

A) The Capan1 pancreatic adenocarcinoma cell line has a deletion at position 6174. **B)** Capan1 and heterogeneous population of olaparib resistant Capan1 (Capan1-OR-Het) cells were plated on 24-well plates, treated with indicated doses of olaparib, and subjected to colony formation after 12 days. Representative images of colony formation are shown. **C)** Dose response curve was calculated with Capan1 (gray) and Capan1-OR-Het (black). Calculated IC50 values with 95% Confidence Intervals (CI) are indicated. **D)** Same as B, but examined the sensitivity to a DNA damaging agent, cisplatin, in Capan1and Capan1-OR-Het cells. Cells were treated with indicated doses. Representative images of foci formation assay are shown. **E)** Same as C, but a cisplatin dose response curve for Capan1 (gray) and Capan1-OR-Het (black) was calculated. **F)** Same as B, but sensitivity to a microtubule stabilization agent, docetaxel, was assessed in Capan1and Capan1-OR-Het cells. Cells were treated with indicated doses. Representative images of foci formation assay are shown. **G)** Same as C, but a docetaxel dose response curve for Capan1 (gray) and Capan1-OR-Het (black) was calculated. **H)** Same as C, but clonal olaparib resistant populations (Capan1-OR-1 [squares] and -2 [triangles]) were isolated and examined for olaparib sensitivity compared to Capan1 cells (circles). Colonies were counted with ImageJ software. Data is representative of 3 independent experiments. Error bars = S.E.M.

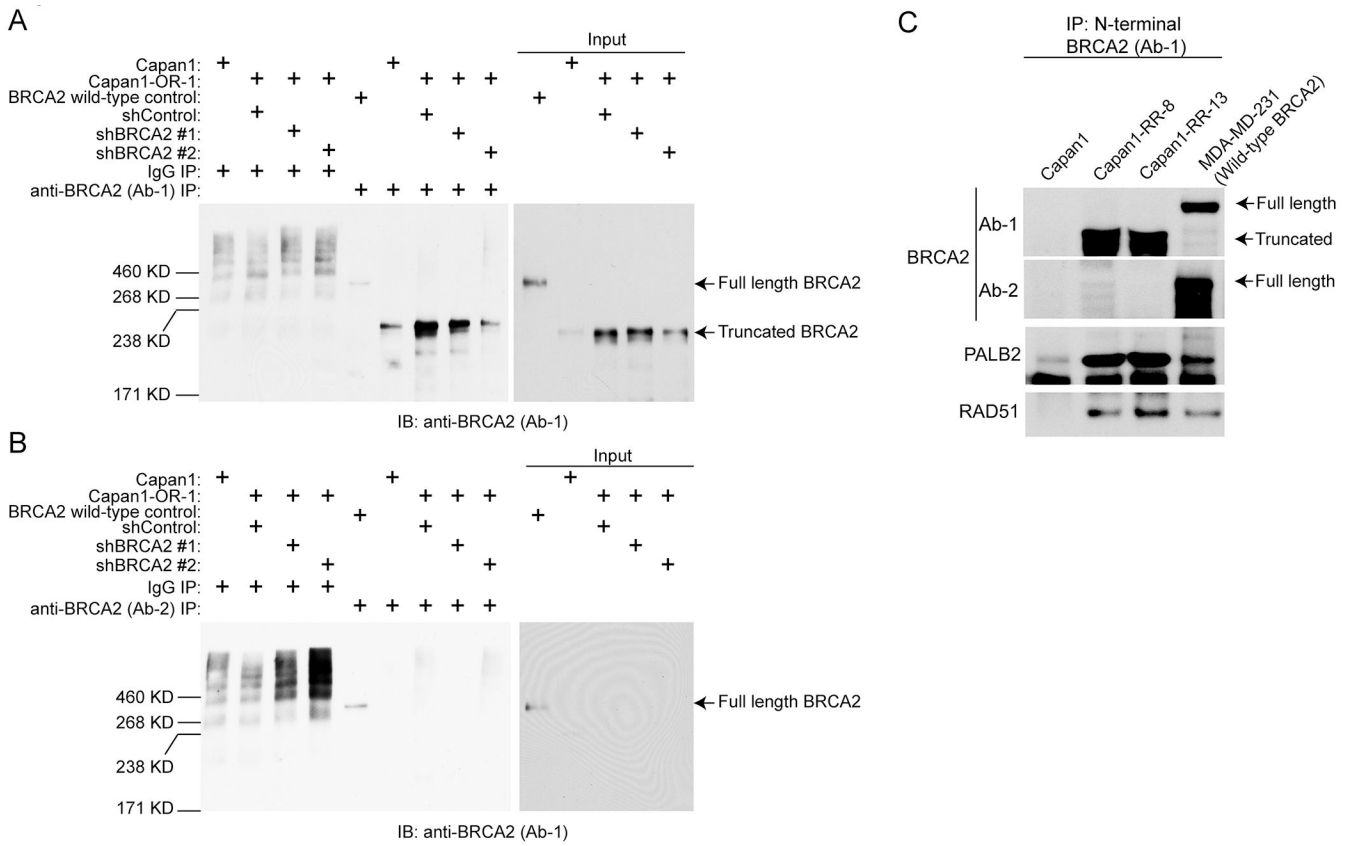

Figure 2. PARP resistant cells express truncated BRCA2.

A) Capan1-OR-1 cells were transduced with shControl and shBRCA2 (#1 and #2). Protein was extracted from Capan1, Capan1-OR-1 (shControl, shBRCA2 #1 and #2) and BRCA2-wildtype control (TOV-21G) cells. Protein was used for immunoprecipitation (IP) against isotype control (IgG) and BRCA2 (N-terminus, Ab-1). IPed protein was used for immunoblot against BRCA2. **B)** Same as A, but IP against BRCA2 (C-terminus, Ab-2). **C)** Nuclear protein was extracted from Capan1, Capan1-RR clones 8 and 13, and a BRCA2-wildtype control. Protein was used for IP against BRCA2 (N-terminus, Ab-1). IP protein was used for immunoblot against BRCA2 (Ab-1 and Ab-2), RAD51, and PALB2.

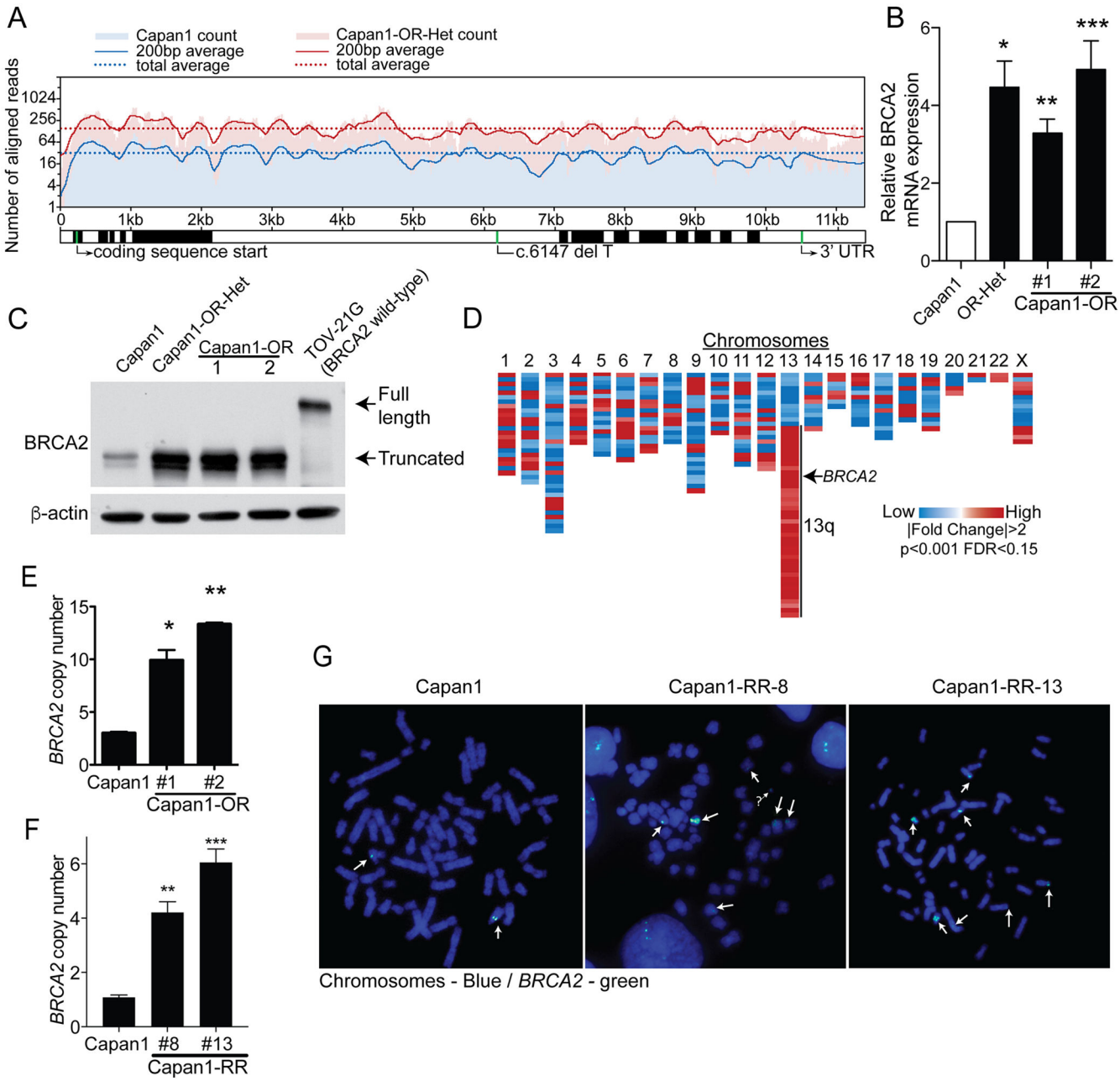

Figure 3. Truncated BRCA2 is overexpressed in CAPAN1 PARP inhibitor resistant cells.

A) Total RNA was isolated from Capan1 and Capan1-OR-Het cells and subsequently used for next generation sequencing (RNA-seq). Aligned-reads for the *BRCA2* gene are shown for Capan1 (parental, blue) and Capan1-OR-Het (resistant, red) cells. **B)** RNA was isolated from Capan1, Capan1-OR-Het, Capan1-OR-1 and 2 and used for qPCR against *BRCA2* (*B2M* = internal control). ANOVA, *p=0.0068, **p=0.007 and ***p=0.0027. **C)** Protein was extracted from Capan1, Capan1-OR-Het, Capan1-OR-1 and 2, and BRCA2-wildtype control (TOV-21G) cells. Protein was immunoblotted against BRCA2 (N-terminus). Arrows indicate full-length and truncated BRCA2. β-actin = loading control. **D)** RNA-seq analysis of Capan1 versus Capan1-OR-Het detected 411 differentially expressed genes (|Fold

Change| >2 and False Discovery Rate [FDR] <0.15). Differentially regulated genes were mapped based on genomic location. **E)** Genomic DNA was isolated from Capan1, CAPAN1-OR-1 and 2 and used for qPCR on *BRCA2* intron-exon junction to determine changes in gene copy number. RNase P = internal control. ANOVA, *p=0.0004 and **p<0.0001. **F)** Genomic DNA was isolated from Capan1, Capan1-RR-8 and 13 and utilized for qPCR *BRCA2* to determine changes in gene copy number. RNase P = internal control. ANOVA, **p=0.0024 and ***p=0.0002. **G**) Fluorescence in situ hybridization against *BRCA2* (green) in Capan1 and Capan1-RR-8 and -13 cells. Chromosomes = DAPI/blue. White arrows = positive *BRCA2* regions. ? = possible extrachromosomal DNA. Data is representative of 3 independent experiments. Error bars = S.E.M.

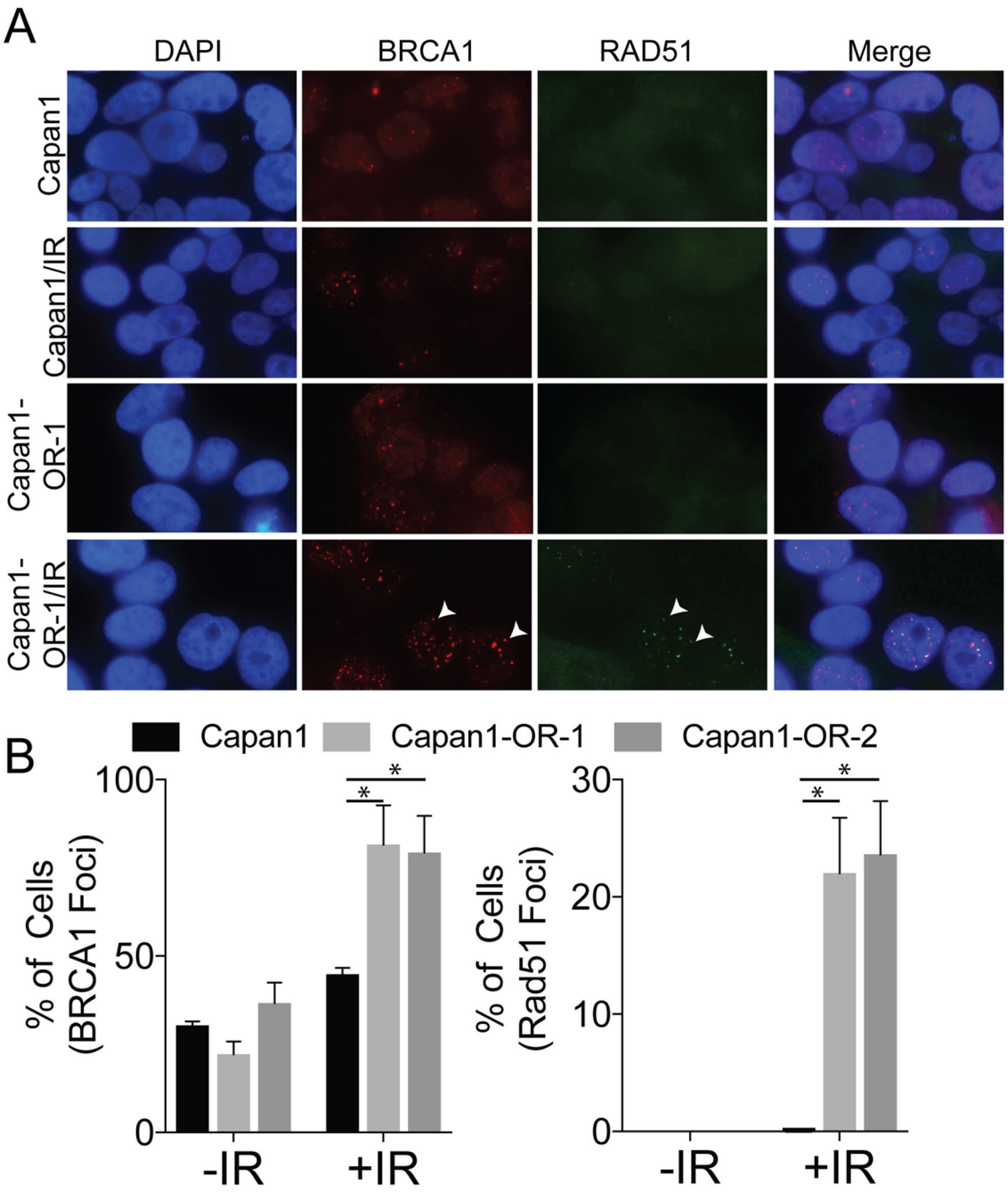

Figure 4. Irradiated PARP resistant cells demonstrate restored homologous recombination DNA repair.

A) Capan1 (parental) and Capan1-OR-1 cells were irradiated (5 Gy) and used for immunofluorescence against BRCA1 (red) and RAD51 (green). White arrowheads indicate BRCA1 and RAD51 foci. **B)** Quantified BRCA1 and RAD51 foci in 200 Capan1, Capan1-OR 1 or 2 cells treated without (−IR) or with (+IR) 5 Gy and graphed as a percentage. Statistical test = ANOVA, *$p < 0.05$. Data is representative of at least 3 independent experiments. Error bars = S.E.M.

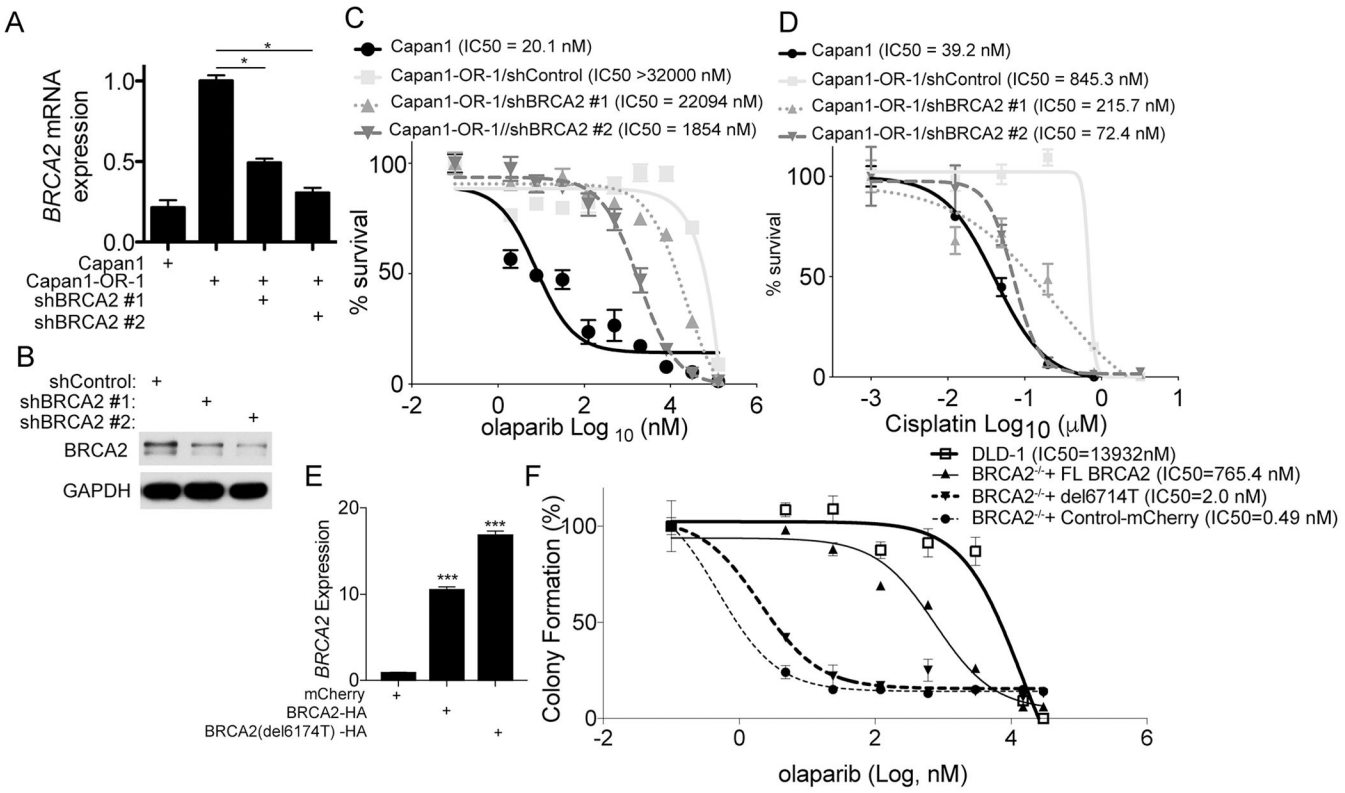

Figure 5. BRCA2 knockdown in CAPAN1-PR cells restores sensitivity to DNA damaging agents.

A) Capan1-OR-1 cells were transduced with shControl or shBRCA2 (#1 or #2). After drug selection RNA was collected and followed by quantitative PCR for *BRCA2*. ANOVA, *p < 0.001. **B)** Same as A, but protein was extracted and immunoblotted for BRCA2. GAPDH = loading control. **C)** Capan1, Capan1-OR-1 shCtrl, or Capan1-OR-1 shBRCA2 (#1 and #2) cells were plated in 24-well plates, treated with increasing doses of olaparib, and cultured for 12 days. Cells were then fixed and used for colony formation assays. Dose response curve shown with indicated IC50 values. **D)** Same as C, but cells were treated with cisplatin. Dose response curve shown with indicated IC50 values. **E)** DLD-1 $BRCA2^{-/-}$ cells were transduced with mCherry or GFP/HA-tagged full length (BRCA2-HA) or truncated BRCA2 (BRCA2(del6174T)-HA). RNA was isolated and *BRCA2* expression was measured via qPCR. ANOVA, ***p< 0.001. **F**) Same as E, but cells were used for a colony formation assay with increasing doses of olaparib. FL = full length. Colonies were counted with ImageJ software. Data is representative of 3 independent experiments. Error bars = S.E.M.

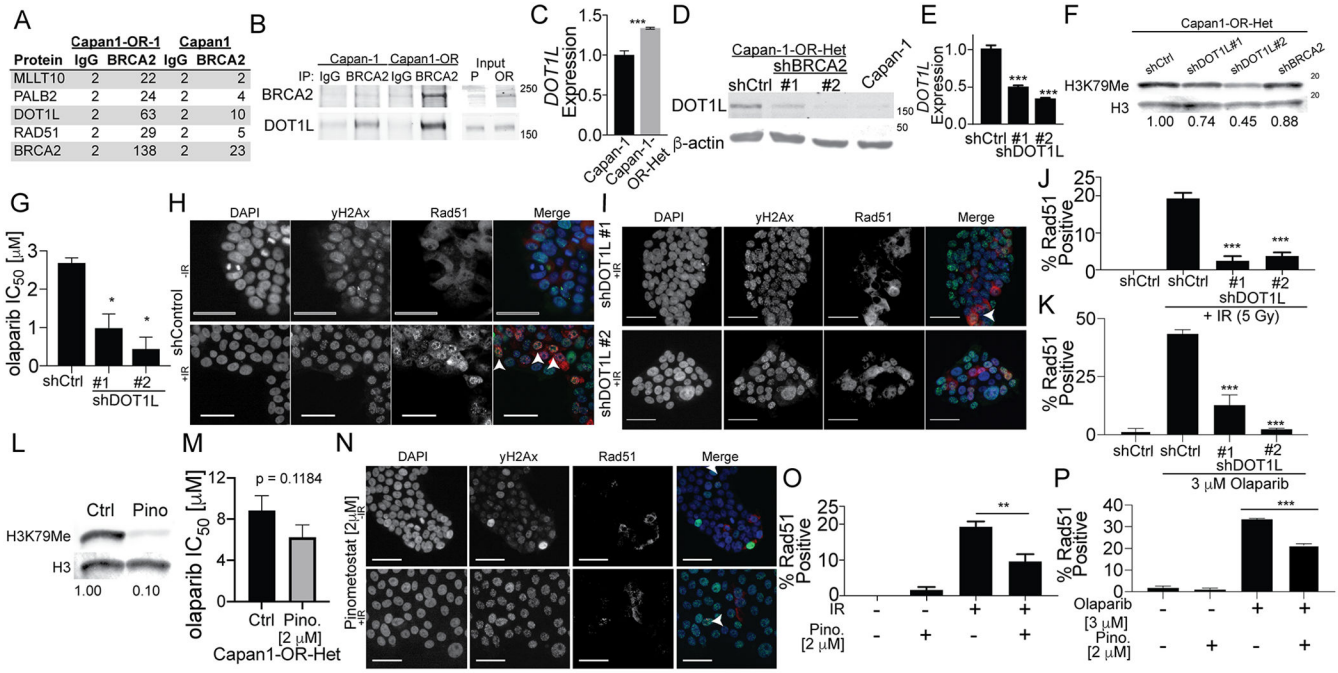

Figure 6. BRCA2 interacts with DOT1L and DOT1L contributes to olaparib resistance.

A) Protein from irradiated (5 Gy, 4 hrs) Capan1-OR 1 cells was used for an immunoprecipitation (IP) against BRCA2 (Ab-1) and isotype control (Rb IgG). IPed protein was separated on a SDS-PAGE and used for mass spectrometry. Peptide count table of Capan1-OR-1 and Capan1 cells. **B)** Capan1 and Capan1-OR-Het cells used for IP against BRCA2 (Ab-1) and isotype control (Rb IgG). IPed protein was separated on a SDS-PAGE and immunoblotted for DOT1L and BRCA2. **C)** RNA extracted from Capan1 and Capan1-OR-Het was used for qPCR against *DOT1L*. Internal control = *B2M*. Two-sided t-test, ***p < 0.001. **D)** Protein from Capan1, Capan1-OR-Het shControl or shBRCA2 (#1 and #2) was separated on a SDS-PAGE and immunoblotted for DOT1L. Loading control = β-actin. **E)** Capan1-OR-Het cells were transduced with a control shRNA (shCtrl) and two *DOT1L* specific-shRNAs (#1 and #2). RNA was extracted from cells and used for qPCR against *DOT1L*. Internal control = *B2M*. ANOVA, ***p < 0.001. **F)** Total histones were extracted and immunoblotted for H3K79Me. Loading control = Histone H3 (H3). **G)** Capan1-OR-Het shCtrl and shDOTL1 (#1 and #2) cells were used for an olaparib dose response colony formation. IC50 were calculated and graphed. ANOVA, *p < 0.05. **H)** Immunofluorescence (IF) on non-irradiated (−IR) and irradiated (5 Gy, +IR) Capan1-OR-Het cells against γH2Ax (green) and RAD51 (red). White arrowheads = RAD51-foci positive cell. **I)** Same as I, but examined Capan1-OR-Het shDOT1L #1 and #2 cells. **J)** Quantification of RAD51-foci positive cells of H and I. At least 200 cells were counted in triplicate. ANOVA, ***p < 0.001. **K)** Capan1-OR-Het shCtrl and shDOTL1 (#1 and #2) cells incubated with olaparib [3 μM for 48 hrs] used for IF against RAD51. At least 200 cells were counted in triplicate. ANOVA, ***p < 0.001. **L)** Capan1-OR-Het cells treated with vehicle control (Ctrl) or 2 μM pinometostat (Pino). Histones were extracted and immunoblotted for H3K79Me. Loading control = Histone H3. **M)** Capan1-OR-Het shCtrl cells were treated with vehicle control or 2 μM pinometostat and cells were used for an olaparib dose response colony formation. IC50

were calculated and graphed. P-value calculated with a two-sided t-test. **N)** Non-irradiated (−IR) and irradiated (5 Gy, +IR) Capan1-OR-Het cells treated with pinometostat [2 μM]. IF against γH2Ax (green) and RAD51 (red). White arrowheads = RAD51-foci positive cell. **O)** Quantification of RAD51-foci positive cells. At least 200 cells were counted in triplicate. ANOVA, **p < 0.01. **P)** Capan1-OR-Het shCtrl cells were treated with vehicle control or 2 μM pinometostat followed by olaparib [3 μM for 48 hrs] used for IF against RAD51. Quantification of RAD51-foci positive cells. At least 200 cells were counted in triplicate. ANOVA, ***p < 0.001. Data is representative of 3 independent experiments. Colony formation was quantified by dissolving crystal violet. Error bars = S.E.M.

Table 1.

Examination of *BRCA2* mutations in The Cancer Genome Atlas.

BRC repeats = RAD51 binding domains.

		Mutations beyond BRC Repeats		Mutations Predicted to Result in Truncated BRCA2 with intact BRC repeats	
Total Patients with *BRCA2* Mutation	# of Cancer Types Examined	# of patients (%)	# of Cancer Types	# of patients (%)	# of Cancer Types
458	45	269/458 (58.7)	35	54/458 (11.8)	20